Carbohydrate Polymers 111 (2014) 198–205

Contents lists available at ScienceDirect

Carbohydrate Polymers

journal homepage: www.elsevier.com/locate/carbpol

Ion exchange kinetics of magnetic alginate ferrogel beads produced by external gelation

Vânea Ferreira Torres Teixeira[a], Nádia Rosa Pereira[a,*], Walter Ruggeri Waldman[b], Ana Luiza Cassiano Dias Ávila[a], Victor Haber Pérez[a], Rubén Jesus Sánchez Rodríguez[c]

[a] Laboratory of Food Technology, Agricultural Science and Technology Center, Northern Rio de Janeiro State University (UENF), Campos dos Goytacazes, Rio de Janeiro, Brazil
[b] Department of Physics, Chemistry and Mathematics, Federal University of São Carlos (UFSCar), Sorocaba, São Paulo, Brazil
[c] Laboratory of Advanced Materials, Science and Technology Center, Northern Rio de Janeiro State University (UENF), Campos dos Goytacazes, Rio de Janeiro, Brazil

ARTICLE INFO

Article history:
Received 27 August 2013
Received in revised form 11 March 2014
Accepted 7 April 2014
Available online 18 April 2014

Keywords:
Diffusion
Encapsulation
Biopolymer
Thermal degradation
Biocatalyst support material

ABSTRACT

This paper reports on a study of the influence of sodium alginate concentration and iron addition on the ion exchange kinetics of calcium alginate ferrogel beads produced by external gelation. The calcium absorption and sodium release of the beads were fitted to Fick's second law for unsteady state diffusion in order to obtain the effective diffusion coefficients of Na^+ and Ca^{2+}. The dried beads were characterized concerning their thermal stability, particle size distribution and morphology. The gelation kinetics showed that an increase in alginate concentration from 1% to 2% increased the Ca^{2+} equilibrium concentration, but presented no effect on Ca^{2+} effective diffusion coefficient. Alginate concentration higher than 2% promoted saturation of binding sites at the bead surfaces. The addition of iron promoted faster diffusion of Ca^{2+} inside the gel beads and reduced the Ca^{2+} equilibrium concentration. Also, iron particles entrapped in the alginate gel beads promoted greater absorption of water compared to pure alginate gel and lower thermal stability of the beads. The main diffusion of Ca^{2+} into and Na^+ out from the bead took place during the first 60 min, during which almost 85–90% of the Ca^{2+} equilibrium concentration is achieved, indicating that this period is sufficient to produce a Ca-alginate bead with high crosslinking of the polymer network.

1. Introduction

The biopolymer alginate is a high molecular weight linear polymer composed of β-D-mannuronic and α-L-guluronic acids (Haug, 1961) and occurs abundantly in brown algae. Alginate solutions are able to form gels due to the polymer structure and their high affinity and binding capacity for polyvalent cations. The gel formation is a result of the crosslinking of divalent cations between the polymer chains, bringing about a three-dimensional lattice structure, according to the egg box model (Davis, Volesky, & Mucci, 2003; Thu, Smidsrød, & Skjåk-Bræk, 1996). Alginate's ability to form gels with simple methods in mild conditions and at low cost causes its widespread application in immobilization and encapsulation of enzymes, proteins and controlled release of drugs (Grant, Morris, Rees, Smith, & Thom, 1973; Ikeda, Takemura, & Ono, 2000; King, 1983; Poncelet & Neufeld, 1996).

In recent years, there has been growing interest in the application of alginate gels as support materials for biocatalyst production, by means of entrapment of whole cells or enzymes in the polymer hydrogel because this makes the catalysts more stable and easily reusable. Also, alginate can be applied as sorbent material for metal uptake in effluent treatments since it has high affinity for metal ions both in the gel and dried state (Davis et al., 2003; Haug, Larsen, & Smidsrød, 1967; Papageorgiou et al., 2006; Vijaya, Popuri, Boddu, & Krishnauah, 2008).

Because of alginate gels' versatility, there is also growing research about alginate ferrogels with magnetic properties, by means of incorporation of metallic iron or magnetite into the gel network. These materials have shown promising applications due to the magnetic properties achieved, such as easy separation of hazardous fluids, accelerated drug release and production of catalysts for biotechnological reactions assisted by magnetic fields (Holland & Yamaura, 2009; Hristov, 1996; Zhao et al., 2011).

* Corresponding author. Tel.: +55 22 2748 6515; fax: +55 22 2739 7194.
E-mail addresses: nadiar@uenf.br, nadiarosa@gmail.com (N.R. Pereira).

http://dx.doi.org/10.1016/j.carbpol.2014.04.009
0144-8617/

The scientific literature contains a large number of papers about the process of forming alginate gels focusing on their properties and ion binding capacity. The gelation mechanism of alginate solutions, mainly sodium alginate, takes place by ionic exchange between Na^+ and Ca^{2+}, when the alginate solution comes into contact with a solution containing Ca^{2+} ions. The achievement of complete gelation is of great importance to guarantee the strength and resistance of the gel. During the gel formation the exchanging of ions itself can impose resistance to cation migration inward and outward the alginate particles. The knowledge about the ion's behavior and operational conditions needed to achieve the maximum ion exchange, with or without magnetic materials, is of great importance on process design, control of polymer characteristic and cost evaluation, concerning industrial production of pure alginate or its derived particles. However, there is no consensus about the conditions and time needed to reach complete gelation of alginate beads. There are many factors that affect this phenomenon, such as the molar mass distribution, the ratio between the mannuronate and guluronate monomers, the aqueous alginate solution concentration, the concentration and nature of crosslinking agents and the preparation method (Blandino, Macias, & Cantero, 1999; Chan, Lee, & Heng, 2006; Liu et al., 2002; Thu et al., 1996), as well as the influence of iron or magnetite addition in the gel formation in the case of ferrogel beads. It is not clear in the literature so far if increasing the concentration of alginate above certain limit would increase the strength and mechanical and thermal resistance of gel beads. In this sense, this work brings contribution to scientific literature about the behavior of ion exchange during the production of alginate gel beads by external gelation method at different alginate concentration and addition of iron particles in alginate network. The ionic exchange was modeled considering the diffusion mechanism for calcium and sodium ions, to describe the conditions needed to reach maximum crosslinking of polymer network. Also, the dried beads were characterized concerning their thermal stability, particle size distribution and morphology.

2. Materials and methods

2.1. Materials

Commercial grade sodium alginate (Protanal LF 20/40) with molecular weight of 200,000–400,000 g mol^{-1}, viscosity of 198 mPa s (1% (w/v) aqueous solution at 20 °C) and pH of 6.7 was provided by FMC Biopolymers. Dehydrated calcium chloride and metallic iron powder were from Sigma–Aldrich.

2.2. Methods

2.2.1. Preparation of calcium alginate beads by dripping technique

The alginate beads were produced in a system consisting of a 5 mm internal diameter stainless steel nozzle with a conical end with 0.7 mm internal diameter connected to a peristaltic pump (Cole-Parmer 7553-70, MasterFlex, USA). The aqueous sodium alginate solutions were prepared at 1%, 2% and 3% (w/w) with constant agitation and treated with ultrasound afterward (USC 1450, Unique, Brazil) at 40 kHz and 100 W during 20 min to release air bubbles. The alginate solution was pumped for drop-wise extrusion into a 0.1 M $CaCl_2$ solution under stirring at 25 °C. Three distances between the nozzle outlet and the surface of the $CaCl_2$ solution were tested: 180, 240 and 300 mm.

Preliminarily, we observed that the lower the alginate flow rate, the more spherical and uniform the gel beads produced were. Therefore, adjustments of the pumping flow had to be made for each concentration of sodium alginate solution in order to guarantee the production of drops instead of continuous flow. Alginate solutions at 1%, 2% and 3% (w/w) were pumped to the dripping nozzle at volumetric flows of 4.2, 3.0 and 1.7 mL min^{-1}, respectively.

The gel beads were dried by natural convection in a thermostatic oven (MA033, Marconi, Brazil) at 100 °C until equilibrium moisture was reached. The dried beads were analyzed for size distribution, morphology and thermal stability.

2.2.2. Preparation of calcium alginate beads with entrapped iron

Metallic iron powder was dispersed in the 2% (w/w) sodium alginate solution at concentrations of 0.2%, 0.4% and 0.6% (w/v). The concentration of 0.6% was chosen for the study of gelation kinetics based on tests conducted in a magnetically assisted reactor that achieved good fluidization of the beads with a low external magnetic field (6 mT) (Teixeira, 2011).

The metallic powder was dispersed in aqueous alginate solution using ultrasound treatment during 10 min at room temperature in an ultrasound water bath at 40 kHz and 100 W (USC 1450, Unique, Brazil). The beads were produced as described in Section 2.2.1 by the dripping technique.

2.2.3. Gelation kinetics

The gelation kinetics of the alginate gel beads was determined by measuring the temporal evolution of Ca^{2+} and Na^+ concentrations after immersion in the $CaCl_2$ solution. The cation concentrations of the beads were determined at 10, 20, 30, 45, 60, 120, 180, 240, 300 and 1440 min of immersion time. A set of 20 beads (1–2 g of sodium alginate solution) was produced in 50.0 mL of $CaCl_2$ solution individually for each immersion time in order to guarantee the production of the beads for the same period. Afterwards, the beads were removed from the crosslinking solution and extensively rinsed with distilled water. Then the beads were weighted and submitted to wet digestion in nitric acid (65%) and hydrogen peroxide mixture (solution) with heating. After digestion, 1 mL of the solution was diluted in water up to 50.0 mL. Five milliliter of 1% lanthanum chloride was also added to reach a solution with final lanthanum concentration of 0.1% (w/v) (according to the AOAC method 990.08 (1998) with modifications). The cations concentrations were determined by atomic absorption spectrometry (AAS-4, Carl Zeiss, Germany), being the Ca^{2+} ion detected by atomic absorption mode and Na^+, by atomic emission mode. All the analyses were carried out in triplicate.

The calcium absorption and sodium release of the beads were analyzed by the diffusion theory concerning the concentration gradient of Ca^{2+} and Na^+ between the two media (alginate beads and $CaCl_2$ solution). Considering unidirectional diffusion in a sphere with homogeneous structure, constant dimensions and constant diffusivity, Fick's second law for unsteady state diffusion yields the following solution (Eq. (1)), assuming uniform initial cation concentration, symmetry of concentration, and surface cation concentration equal to the equilibrium concentration:

$$\frac{C_A - C_A^{eq}}{C_A^0 - C_A^{eq}} = \frac{6}{\pi^2}\sum_{n=1}^{\infty}\left(\frac{1}{n}\right)^2 \exp\left(-\left(\frac{n\pi}{R}\right)^2 D_{ef}t\right) \quad (1)$$

where C_A corresponds to the concentration of Ca^{2+} or Na^+ ions at time t, C_A^{eq} is the concentration of the ions at equilibrium and C_A^0 is their initial concentration, R is the average radius of the spheres (2.25 mm) and D_{ef} is the effective diffusivity of the Ca^{2+} or Na^+ ions.

For long diffusion time, it is acceptable to truncate the series at the first term, yielding the general solution for Ca^{2+} and Na^+ as follows:

$$C_{Ca} = C_{Ca}^{eq} - C_{Ca}^{eq}\exp\left(-\frac{\pi^2}{R^2}D_{ef}t\right) \quad (2)$$

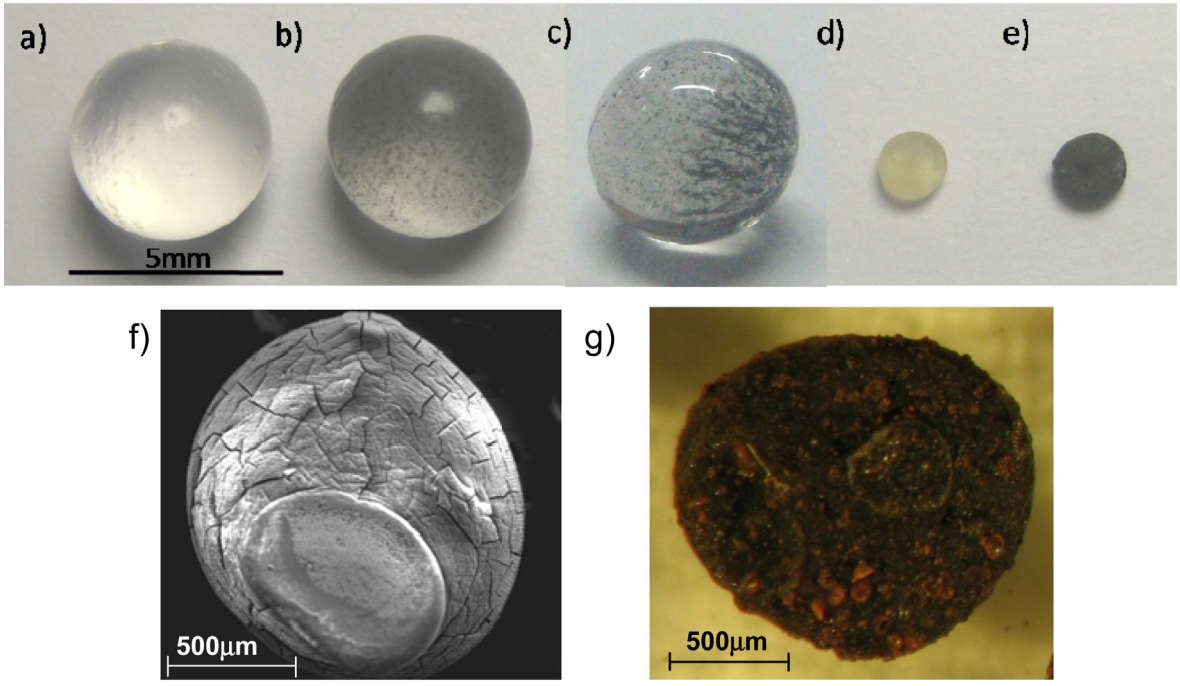

Fig. 1. Calcium alginate beads produced by dripping method: pure alginate in the gel state (a), with 0.6% iron dispersed produced by manual stirring (b) and with magnetic stirring (c) and after air drying in oven at 100 °C – pure alginate (d), with addition of 0.6% of iron (e), SEM image (magnification ×56) of dried pure alginate (f) and stereoscopic image of dried alginate with addition of 0.6% of iron (g). (For interpretation of reference to color in text, the reader is referred to the web version of this article.)

$$C_{Na} = C_{Na}^{eq} + C_{Na}^{0} \exp\left(-\frac{\pi^2}{R^2} D_{ef} t\right) \quad (3)$$

The data of Ca^{2+} and Na^{+} concentration measured in the alginate beads after immersion in the $CaCl_2$ solution for different time intervals were fitted by nonlinear curve fitting to Eqs. (2) and (3), respectively, and the parameter D_{ef} was determined for each cation.

2.2.4. Thermal stability

Thermogravimetric analysis (TGA) was used to characterize the calcium alginate beads with and without the incorporation of iron. Analyses were conducted using an SDT 2960 thermogravimetric system (TA Instruments) with sensitivity of 0.1 μg. The dried samples (around 16.0 mg) were analyzed under a dynamic atmosphere of nitrogen with a flow of 100 mL min^{-1} between 20 and 1150 °C, with a heating rate of 20 °C min^{-1}. The data were processed using the V3 Universal System Analysis software (TA Instruments).

2.2.5. Morphological analysis

The analysis of the dried beads' morphology was performed using optical microscopy (OM) and scanning electron microscopy (SEM). The optical microscopic images of dried beads placed in a Petri dish were obtained with a stereoscopic microscope with digital camera attached (Eclipse E-200, Nikon). For the SEM images, the dried samples were mounted on aluminum stubs and sputtered with metallic gold for be observed and photographed under a Shimadzu SSX-550 scanning electron microscope.

2.2.6. Size distribution analysis

The size distribution of the dried calcium alginate beads, with and without addition of iron, was determined with a Shimadzu SALD-3101 laser diffraction particle analyzer.

Table 1
Shape of alginate beads according to the operational conditions of dripping production.

Alginate concentration (% w/w)	Distance (mm)[a]	Shape
1%	180	Spherical
	240	Spherical
	300	Flat
2%	180	Tail formation
	240	Spherical
	300	Flat
3%	180	Tail formation
	240	Spherical
	300	Flat

[a] Distance between the nozzle outlet orifice and the surface of $CaCl_2$ solution.

3. Results and discussion

3.1. Formation of calcium alginate gel beads

The calcium alginate beads were spherical, with diameter in the range of 4–5 mm and white color. The gel beads are formed by the external gelation mechanism, by which good size and shape uniformity can be achieved (Chan et al., 2006; Fundueanu, Nastruzzi, Carpov, Desbrieres, & Rinauto, 1999), as can be seen in Fig. 1.

Considering the influence of distance between the nozzle outlet and the surface of calcium chloride solution and the concentration of alginate solution, the former had the greatest influence on the shape of gel beads. Beads with short tails were obtained for the lowest distance (180 mm) for 2% and 3% sodium alginate concentration (Table 1). An increase in the distance of the drop trajectory to 240 mm changed the drops' shape to a more spherical one. However, an increase in the distance to 300 mm led to the production of ellipsoidal beads and smaller satellite beads (on the order of microns) for all alginate solutions. The increase in travel distance of the drop promotes an increase in the drop velocity, which causes compression of the drops, flattening the gel beads. This increase in

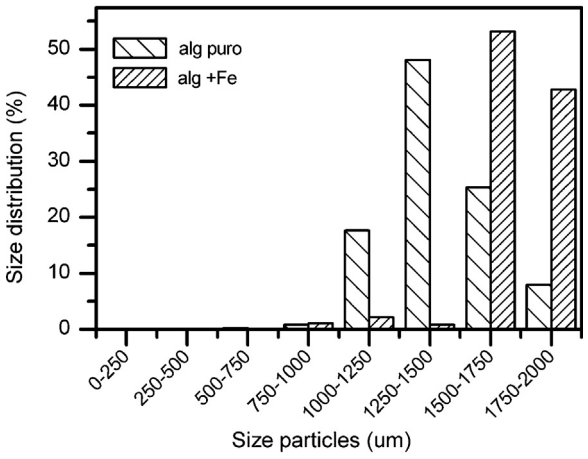

Fig. 2. Beads size distribution for 2% alginate air dried beads with and without addition of 0.6% of iron.

velocity also splits up the drop to some extent when it comes in contact with the gelation solution, forming micro-size beads along with the main drop.

In general, the dried beads presented great shrinkage (Fig. 1d) and lost their spherical shape to some extent in comparison to the gel beads. However, the latter effect was stronger for dried beads produced with alginate solution concentration of 1%, probably due to lower gel resistance of such particles (Papageorgiou et al., 2006). The dried beads presented narrow size distribution, with 97–99% of the diameters in the range of 1–2 mm (Fig. 2). The incorporation of iron in the alginate beads slightly increased their diameter. This may be due to non-shrinking behavior of iron particles in the alginate network, which reduced the beads' shrinkage during drying.

The alginate ferrogel beads, produced under the same conditions as described for pure alginate with and without dispersion of metallic iron, presented similar characteristics. The incorporation of iron is attractive because it provides magnetic properties to alginate gel, allowing application of alginate beads in magnetic systems, such as magnetically assisted reactors and as supports for drug delivery systems with some magnetic driven properties (Zhao et al., 2011). The metallic iron was homogenously dispersed in the alginate solution (Fig. 1b), but it was important to maintain stirring to avoid settlement over time. The dispersion is easily achieved compared to dispersion of iron oxide nanoparticles (data not shown), which need to be precoated to minimize agglomeration and improve gel homogeneity (Zhao et al., 2011). We observed the alignment of iron when magnetic agitation was used during the gel beads' production, as can be seen in Fig. 1c. Therefore, manual stirring has to be used instead in order to achieve homogeneous distribution of iron in the gel beads. Also, this observation brings information about the iron mobility in the gel beads, indicating that the gel state of such beads may present operational problems in magnetically assisted systems. In contrast, the dried beads had a more rigid structure, probably reducing the iron mobility inside the beads.

The alginate beads were air dried by natural convection at 100 °C and observed by scanning electron microscopy. Fig. 1f illustrates the micrograph of a 2% alginate dried bead. It can be observed that drying influenced the bead morphology concerning the surface characteristics and size. The dried alginate bead surface presents an organized structure with parallel lines and some fissures. This suggests cracking of the polymer network, probably due to tensions promoted by shrinking during drying. The same behavior was observed by Fundueanu et al. (1999).

The addition of metallic iron promoted a less smooth surface of the dried alginate beads by means of projected iron agglomerates on the bead surface (Fig. 1g). Also, some red spots can be seen on the external surface of the bead, indicating iron oxidation during immersion in the $CaCl_2$ solution or drying process. An increase in iron concentration in the alginate bead intensified the color of these red spots and increased their number. Additionally, there was a change in the color of chloride solution from white to red and some rust incrusted on the wall of the immersion vessel for the samples produced with iron concentration higher than 0.8% (w/v) (data not shown).

3.2. Gelation kinetics of pure alginate beads

Most experimental studies in the literature have produced Ca-alginate beads by external gelation within 60 min of immersion time in $CaCl_2$ solution. We considered important to estimate at what stage of gelation were our samples at this time of immersion. Furthermore, kinetics data was studied in order to estimate the maximum gelation time needed to achieve complete gelation of alginate particles.

In order to follow the completion of alginate gel beads gelation, we measured the Ca^{2+} and Na^{+} concentrations of the beads produced with alginate solution at 1%, 2% and 3% during different immersion times in the $CaCl_2$ solution. Fig. 3 shows the kinetics of Ca^{2+} absorbed by and Na^{+} released from the alginate matrices. The Ca^{2+} concentration increased steeply during the first 30 min of the process. After that period, the rate of cation migration decreased and the Ca^{2+} concentration tended to equilibrium, reaching a plateau around the cation equilibrium concentration ($C^{eq}_{Ca^{2+}}$). This indicates an intense diffusion mechanism of calcium at the beginning of the gel formation, mainly because of the higher concentration gradient between the alginate drop and the chloride solution as well as the higher availability of electronegative cavities of the G-blocks. A gel film is formed in the external region of the bead as long as the calcium ions extensively bond to guluronic acid blocks at the drop surface (Thu, Skjåk-Bræk, Micali, Vittur, & Rizzo, 1997). Therefore, a more rigid net was formed, with a film at the surface that was less permeable to inward diffusion of calcium (Chan et al., 2006; Liu et al., 2002).

On the other hand, almost all the Na^{+} of the alginate solution was released during the gelation process, reaching equilibrium concentrations at very low values, varying as a function of alginate concentration, as discussed after in text (Fig. 3b). The higher the alginate concentration was, the faster the equilibrium concentration was reached. This phenomenon took place because there is a favorable gradient to Na^{+} displacement from alginate monomers and by the smaller atomic size of Na^{+} ion compared to Ca^{2+} one. Therefore, the former diffused faster and almost all Na^{+} was released before the Ca^{2+} crosslinking with alginate carboxylic guluronic groups (or G blocks) promoted a denser polymer network structure, which might impose higher resistance to sodium release.

Taking into account that both cations' migration is governed by the diffusion mechanism, the effective diffusion coefficients of Ca^{2+} and Na^{+} were obtained by fitting the cation concentration data to Eqs. (2) and (3). Both models presented good fit to the experimental data, as can be seen in Fig. 3. As shown in Table 2, an increase of alginate concentration from 1% to 3% showed no statistically relevant difference in the effective Ca^{2+} diffusion coefficient. On the other hand, an increase of alginate concentration from 1% to 2% boosted the Ca^{2+} equilibrium concentration, but the same was not observed for an increase of alginate concentration from 2% to 3%.

Higher polymer concentration means more polymer molecules per unit of volume and consequently more binding sites to crosslink with Ca^{2+} ions. However, it has been suggested that the crosslink between Ca^{2+} and carboxyl groups takes place first at the matrix surface, since it is the first point of contact, as commented later

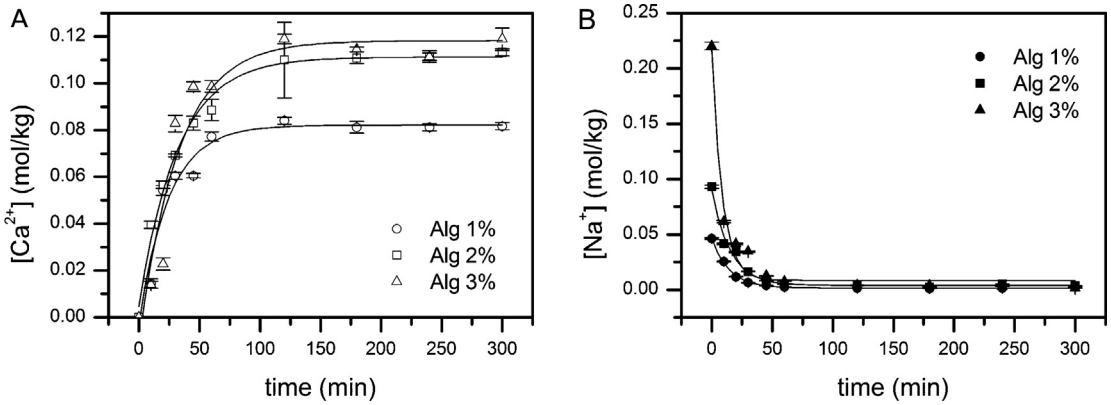

Fig. 3. Ca^{2+} concentration (a) and Na^{+} concentration (b) during gelation process of alginate gel beads produced by dripping method.

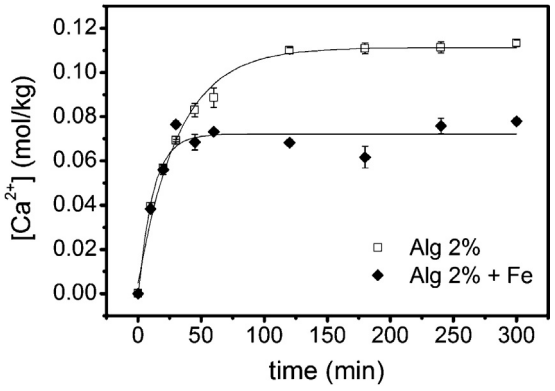

Fig. 4. Ca^{2+} content during gelation process of 2% alginate gel beads with and without 0.6% iron addition produced by dripping method.

(Chan et al., 2006). Consequently, an increase in alginate from 1% to 2% promotes an increase in electronegative cavities of G-blocks, providing more crosslinkage with Ca^{2+} ions and consequently an increase in Ca^{2+} concentrations in the beads (Fig. 3 and Table 2). However, although an increase of alginate concentration from 2% to 3% increased the binding sites, there was no increase of Ca^{2+} concentration as observed between alginate concentrations of 1% and 2%. This can be attributed to the irreversible gelation that occurs due to higher concentrations of alginate. The diffusion rate of the alginate toward the gelling zone is directly proportional to its concentration, and the higher the rate of diffusion, the higher is the concentration gradient between the surface and the bulk of the gel (Skjåk-Bræk, Grasdalen, & Smidsrod, 1989). Therefore, there was no significant difference of the effective Ca^{2+} diffusion coefficient of the polymer (Table 2). This suggests that increased gelation of the bead surface for alginate concentration higher than 2% decreases the rate of calcium migration into the gel.

In the case of Na^{+} release from the alginate solution, the higher the alginate concentration, the higher the Na^{+} effective diffusivity. On the other hand, as the alginate concentration increased, the Na^{+} equilibrium concentration increased. Therefore, some resistance to Na^{+} diffusion occurs, probably by the more compact structure promoted by higher crosslinking of alginate G-blocks with Ca^{2+}.

As can be seen in the kinetics curves of Ca^{2+} concentration, the main calcium diffusion in the biopolymer chain takes place during the first 60 min, during which almost 85–90% of the Ca^{2+} equilibrium concentration is achieved in the beads for all alginate concentrations. Therefore, these results prove that such time can be taken as not sufficient to completion of alginate gelation. However, it still produces Ca-alginate beads with enough mechanical stability to allow handling and working in the studied conditions, since mechanical and thermal properties are function of calcium concentration of the polymer chain (Blandino et al., 1999; Chan et al., 2006; Fundueanu et al., 1999; Liu et al., 2002; Pathak et al., 2010).

3.3. Gelation kinetics of alginate beads with entrapped iron

Fig. 4 illustrates the Ca^{2+} absorption kinetics for alginate beads produced with 2% alginate solution with and without inclusion of 0.6% iron. It can be observed that the presence of iron influenced the gelation kinetics of the beads. The Ca^{2+} equilibrium concentration decreased from 0.111 to 0.072 mol/kg when iron was added to the alginate solution (Table 2) and also the time needed to reach equilibrium decreased, from 120 min to 60 min. The iron addition increased the Ca^{2+} and Na^{+} effective diffusion coefficients. The Ca^{2+} effective diffusion coefficient of alginate ferrogels was 2.6-fold higher than pure alginate gel beads, and was the highest of all other experimental conditions. This may be due to the formation of paths in the polymer network, facilitating the diffusion mechanism. On the other hand, the increase in Na^{+} effective diffusion coefficient was less pronounced.

These effects can be explained by competition between calcium and iron ions for polymer binding sites, as alginate also presents chemical affinity for divalent iron (Davis et al., 2003; Perez-Moral, Gonzalez, & Parker, 2013; Smidsrød & Draget,

Table 2
Effective diffusivities and equilibrium concentration of $[Ca^{2+}]$ and $[Na^{+}]$.

Alginate concentration (% w/w)	$[Ca^{2+}]$ absorption			$[Na^{+}]$ release		
	$C^{eq}_{Ca^{2+}}$ (mol/kg)	D_{ef} ($\times 10^{-10}$ m^2/s)	R^2	$C^{eq}_{Na^{+}}$ (mol/kg)	D_{ef} ($\times 10^{-10}$ m^2/s)	R^2
1%	0.082 ± 0.003^{a}	3.5 ± 0.6^{a}	0.96	0.0014 ± 0.0004^{a}	5.9 ± 0.3^{a}	0.997
2%	0.111 ± 0.002^{b}	2.7 ± 0.2^{a}	0.99	0.004 ± 0.002^{ab}	5.6 ± 0.6^{a}	0.99
2% + 0.6% Fe	0.072 ± 0.003^{a}	7 ± 2^{b}	0.94	0.004 ± 0.001^{ab}	6.6 ± 0.6^{a}	0.99
3%	0.118 ± 0.007^{b}	2.7 ± 0.6^{a}	0.93	0.008 ± 0.004^{b}	10 ± 1^{b}	0.99

Average values within a column followed by same superscript letters are not statistically different ($p > 0.05$).

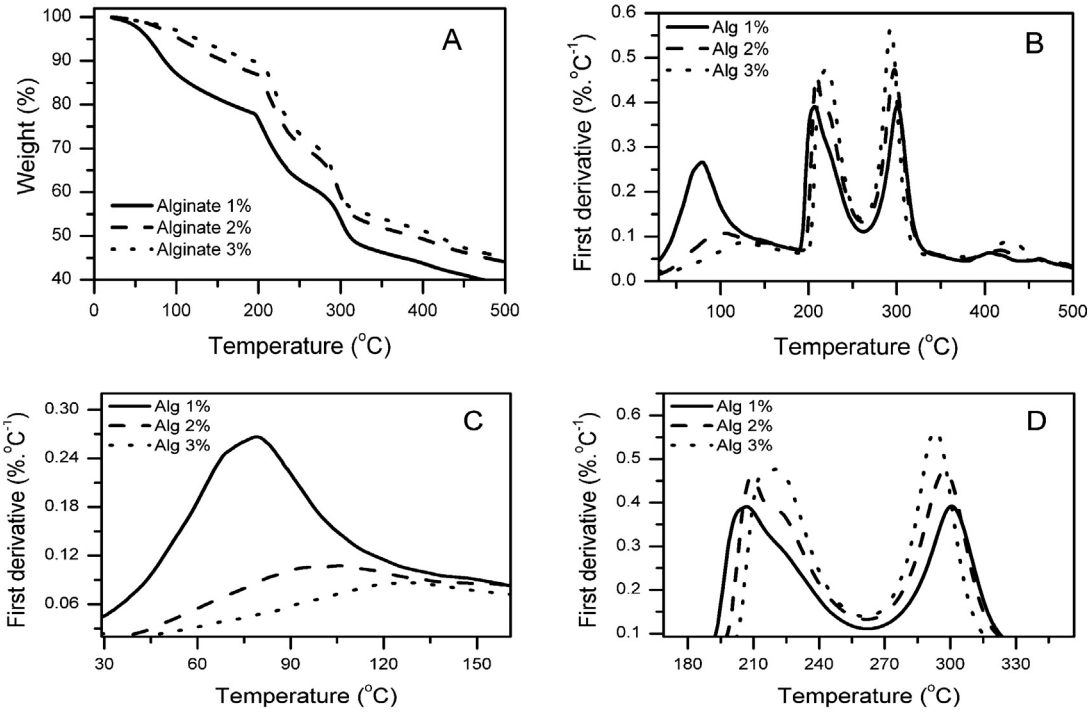

Fig. 5. Thermogravimetric curves obtained for calcium alginate beads produced with sodium alginate solutions at 1%, 2% and 3%: (a) TGA, (b) DTG (all temperature interval), (c) zoom at the first process of weight loss and (d) zoom at the second and third process of weight loss.

1996). As discussed before, some iron oxidation occurred during the preparation of the alginate ferrogel beads, with the production of Fe^{2+}. Therefore, binding of Fe^{2+} with alginate G-blocks may have taken place directly or after ion exchange with Ca^{2+}, decreasing the calcium concentration of the ferrogel beads during the gelation process. On the other hand, the metallic powders entrapped in the three-dimensional lattice of crosslinked polymer can pose physical barriers, causing resistance to Ca^{2+} mobility and to Ca^{2+} crosslinking to the electronegative cavities of G-blocks.

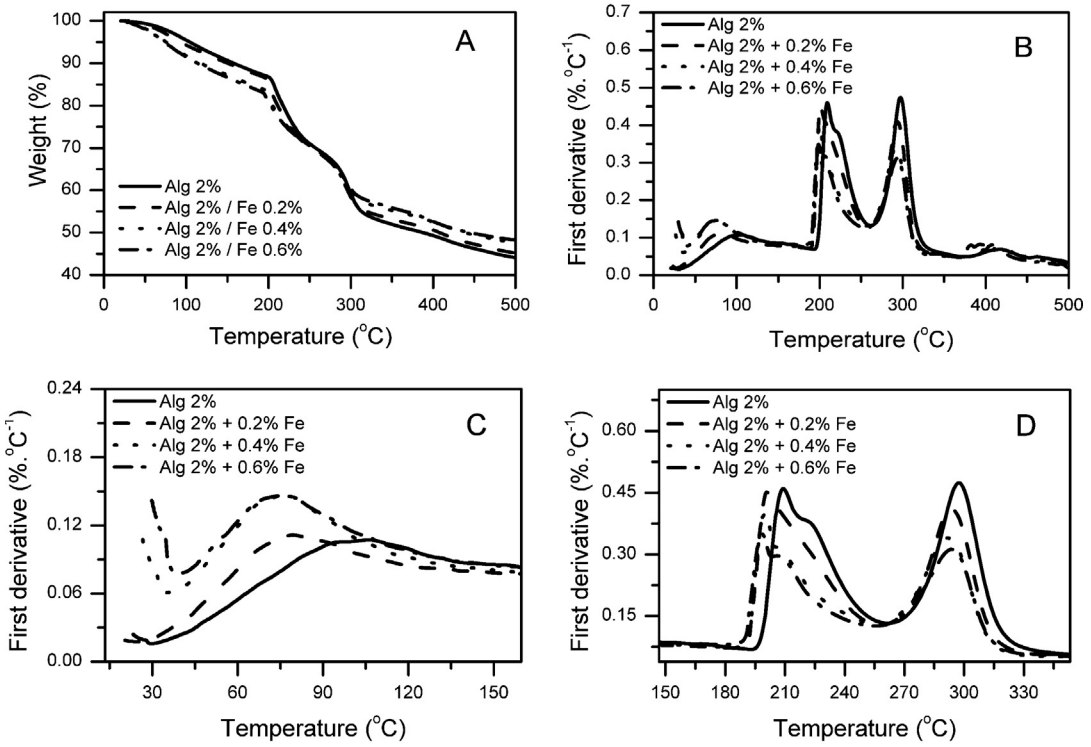

Fig. 6. Thermogravimetric curves obtained for calcium alginate beads produced with 2% sodium alginate solution and with 0%, 0.2%, 0.4% and 0.6% of metallic iron: (a) TGA, (b) DTG (all temperature interval), (c) zoom at the first process of weight loss and (d) zoom at the second and third process of weight loss.

Additionally, the ferrogels alginate beads presented lower resistance to manual squeezing in comparison to the pure alginate beads. This indicates lower mechanical resistance because of iron entrapment in the polymer network.

3.4. Thermogravimetric analysis

The thermogravimetric results for 1%, 2% and 3% alginate beads are illustrated in Fig. 5, which shows three main processes of weight loss (Ross et al., 2011). The first process, from 50 to 200 °C, is related to dehydration of coordinated water molecules and the destruction of glycosidic bonds. The second decomposition process, at 200–260 °C, is associated with depolymerization, leading to the formation of levoglucosan ($C_6H_{10}O_5$), which is further thermodegraded to intermediate substances with low molecular weight, such as oxalates. In the third degradation process, more water and carbon dioxide from the decarboxylation process were generated (Dong, Dong, Cao, Han, & Ding, 2011; Zaafarany et al., 2012; Zhang et al., 2011).

Despite the impression that lower concentrations of calcium alginate are more thermally stable (Fig. 5a), it is possible to observe the limitation of this interpretation by the first derivative of weight loss (Fig. 5b). Indeed, the first weight loss process was a consequence of water evaporation and was not related with thermal degradation of the polymeric chain. The behavior observed for water evaporation is consistent with what is expected for higher concentrations of alginate. As the alginate concentration increased, there was greater approximation between the polymer chains by higher concentration of crosslinks, which reduced the space for water molecules. In the first weight loss process of pure calcium alginate beads, the onset temperature varied as a function of calcium concentration: the higher the concentration of calcium, the higher the onset temperature (Fig. 5c and d). This is probably due to the higher intermolecular interaction between chains, which leads to a more cohesive system. The low cohesion between chains for lower concentrations of alginate is consistent with the behavior observed for water loss.

The TGA results for alginate beads with iron addition are presented in Fig. 6a. The addition of iron particles to calcium alginate interfered in the three weight loss processes. Fig. 6b shows there was greater water content for the alginate with metallic iron particles than when it was pure; with a slight tendency for greater water content, directly proportional to the iron concentration. In Fig. 6b, it is possible to observe a shift of onset temperature of weight loss to lower values of around 10 °C for the second weight loss process, related to the generation and decomposition of oxalates. The second and third weight loss processes showed a change in weight loss inversely proportional to iron content, behavior contrary to the water weight loss process. Probably this behavior took place due to the increased mass of metallic iron in the composite. The apparent effect of the iron content on alginate thermal stability could be associated with iron particles, as can be observed in the first and the second peaks. These particles play a role in the temperature homogenization of samples due to their lower heat capacity and greater thermal conductivity, resulting in lower temperature values for maximum weight loss rate, as observed in Fig. 6c and d. Additionally, one more weight loss process occurred, with effect inversely proportional to the concentration of alginate for temperatures higher than 380 °C (Fig. 6b). We did not find any reports in the literature about the nature of this weight loss process.

4. Conclusions

The results indicate that the production of spherical calcium alginate beads by the dripping method is influenced by the distance between the nozzle orifice and the sodium alginate gelation solution, solution concentration and volumetric flow rate. The addition of metallic iron in the polymer solution produced alginate gel beads with homogeneous iron entrapment in the three-dimensional polymer lattice, with magnetic properties. However, oxidation of iron into the bead varies depending on gelation time and iron concentration.

The gelation kinetics study showed that the sodium alginate concentration influences Na^+ and Ca^{2+} ion exchange, which is governed by the diffusion mechanism. The Ca^{2+} crosslink to polymer monomers took place from the surface toward the center of the beads. An increase in alginate concentration above 2% did not promote higher crosslinkage of alginate monomers with Ca^{2+}, indicating saturation of the binding sites at the gel bead surface.

The gelation mechanism of alginate presented good fit to Fick's second law for unsteady state diffusion. The Ca^{2+} effective diffusion coefficient was not influenced by alginate concentration, but an increase of alginate concentration from 1% to 2% boosted the Ca^{2+} equilibrium concentration. On the other hand, an increase in alginate concentration promoted an increase in Na^+ effective diffusion coefficient and its equilibrium concentration. Also, the main diffusion of calcium into and sodium out from the beads took place during the first 60 min, leading to the conclusion that this time is sufficient to produce Ca-alginate beads with high crosslinkage of the polymer network (around 85–90%), but not sufficient to completion of alginate gelation.

The addition of iron to the gel beads interfered in the gelation kinetics concerning the amount of calcium bound to the polymer network, promoting faster diffusion of Ca^{2+} ions in the gel beads and reducing the Ca^{2+} equilibrium concentration. Also, ion exchange between Ca^{2+} and Fe^{2+}, generated by oxidation of iron at the beads' surface, might have taken place.

The alginate gels presented three main weight loss processes, coherent with the literature: water evaporation, generation and degradation of oxalates and decomposition of more complex structures. The iron addition in the gel network promoted greater absorption of water compared to pure alginate gel and lower thermal stability of alginate beads.

Acknowledgements

We would like to acknowledge the financial support of FAPERJ and CAPES. Also, we are grateful for the support of the laboratories at UENF where the analyses were carried out.

References

AOAC. (1998). (17th ed.). *Official methods of analysis of the AOAC international* (Vol. VII) Gaithersburg: Association of Official Analytical Chemists.

Blandino, A., Macias, M., & Cantero, D. (1999). Formation of calcium alginate gel capsules: Influence of sodium alginate and $CaCl_2$ concentration on gelation kinetics. *Journal of Bioscience and Bioengineering*, *88*(6), 686–689.

Chan, L. W., Lee, H. Y., & Heng, P. W. S. (2006). Mechanisms of external and internal gelation and their impact on the functions of alginate as a coat and delivery system. *Carbohydrate Polymers*, *63*, 176–187.

Davis, T. A., Volesky, B., & Mucci, A. (2003). A review of the biochemistry of heavy metal biosorption by brown algae. *Water Research*, *37*, 4311–4330.

Dong, Y., Dong, W., Cao, Y., Han, Z., & Ding, Z. (2011). Preparation and catalytic activity of Fe alginate gel beads for oxidative degradation of azo dyes under visible light irradiation. *Catalysis Today*, *175*, 346–355.

Fundueanu, G., Nastruzzi, C., Carpov, A., Desbrieres, J., & Rinauto, M. (1999). Physico-chemical characterization of Ca-alginate microparticles produced with different methods. *Biomaterials*, *20*, 1427–1435.

Grant, G. T., Morris, E. R., Rees, D. A., Smith, P. J. C., & Thom, D. (1973). Biological interactions between polysaccharides and divalent cations: The egg-box model. *FEBS Letters*, *32*, 195–198.

Haug, A. (1961). The affinity of some divalent metals to different types of alginates. *Acta Chemica Scandinavica*, *15*(8), 1794–1795.

Haug, A., Larsen, B., & Smidsrød, O. (1967). Correlation between chemical structure and physical properties of alginates. *Acta Chemica Scandinavica*, *21*, 691–704.

Holland, D., & Yamaura, M. (2009). Adsorption of uranyl ions on magnetite nanoparticles. In *4th international nuclear Atlantic conference* Rio de Janeiro, Brazil.

Hristov, J. Y. (1996). Fluidization of ferromagnetic particles in a magnetic field. Part 1: The effect of field line orientation on bed stability. *Powder Technology*, *87*(1), 59–66.

Ikeda, A., Takemura, A., & Ono, H. (2000). Preparation of low-molecular weight alginic acid by acid hydrolysis. *Carbohydrate Polymers*, *42*, 421–425.

King, A. H. (1983). Brown seaweed extracts (alginates). *Food Hydrocolloids*, *2*, 115–188.

Liu, D. X., Yu, W., Zhang, Y., Xue, W. M., Yu, W. T., Xiong, Y., et al. (2002). Characterization of structure and diffusion behavior of Ca-alginate beads prepared with external or internal calcium sources. *Journal of Microencapsulation*, *19*(6), 775–782.

Papageorgiou, S. K., Katsaros, F. K., Kouvelos, E. P., Nolan, J. W., Deit, L. H., & Kanellopoulos, N. K. (2006). Heavy metal sorption by calcium alginate beads from *Laminaria digitata*. *Journal of Hazardous Materials*, *137*(3), 1765–1772.

Pathak, T. S., Yun, J., Lee, J., & Paeng, K. (2010). Effect of calcium ion (cross-linker) concentration on porosity, surface morphology and thermal behavior of calcium alginates prepared from algae (*Undaria pinnatifida*). *Carbohydrate Polymers*, *81*, 633–639.

Perez-Moral, N., Gonzalez, M. C., & Parker, R. (2013). Preparation of iron-loaded alginate gel beads and their release characteristics under simulated gastrointestinal conditions. *Food Hydrocolloids*, *31*, 114–120.

Poncelet, D., & Neufeld, R. J. (1996). Fundamentals of dispersion in encapsulation technology. *Progress in Biotechnology*, *11*, 47–54.

Ross, A. B., Hall, C., Anastasakis, K., Westwood, A., Jones, J. M., & Crewe, R. J. (2011). Influence of cation on the pyrolysis and oxidation of alginates. *Journal of Analytical and Applied Pyrolysis*, *91*(2), 344–351.

Skjåk-Bræk, G., Grasdalen, H., & Smidsrød, O. (1989). Inhomogeneous polysaccharide ionic gels. *Carbohydrate Polymers*, *10*(1), 31–54.

Smidsrød, O., & Draget, K. I. (1996). Chemistry and physical properties of alginates. *Carbohydrate Europe*, *14*, 6–13.

Teixeira, V. F. T. (2011). *Study of obtaining biocatalysts with matrices of calcium alginate in order to produce biodiesel* M.Sc. Dissertation. Brazil: Universidade Estadual do Norte Fluminense (in Portuguese).

Thu, B., Smidsrød, O., & Skjåk-Bræk, G. (1996). Alginates gels – Some structure–function correlations relevant to their use as immobilization matrix for cells. *Progress in Biotechnology*, *11*, 19–30.

Thu, B., Skjåk-Bræk, G., Micali, F., Vittur, F., & Rizzo, R. (1997). The spatial distribution of calcium in alginate gel beads analysed by synchrotron-radiation induced X-ray emission (SRIXE). *Carbohydrate Research*, *297*, 101–105.

Vijaya, Y., Popuri, S. R., Boddu, V. M., & Krishnauah, A. (2008). Modified chitosan and calcium alginate biopolymer sorbents for removal of nickel (II) through adsorption. *Carbohydrate Polymers*, *72*, 261–271.

Zaafarany, I., Khairou, K., Tirkistani, F., Iqbal, S., Khairy, M., & Hassan, R. (2012). Kinetics and mechanism of non-isothermal decomposition of Ca(II)-, Sr(II)- and Ba (II)-cross-linked divalent metal–alginate complexes. *International Journal of Chemistry*, *4*(6), 7–14.

Zhang, J., Ji, Q., Shen, X., Xia, Y., Tan, L., & Kong, Q. (2011). Pyrolysis products and thermal degradation mechanism of intrinsically flame-retardant calcium alginate fibre. *Polymer Degradation and Stability*, *96*, 936–942.

Zhao, X., Kim, J., Cezar, C. A., Huebsch, N., Lee, K., Bouhadir, K., et al. (2011). Active scaffolds for on-demand drug and cell delivery. *Proceedings of the National Academy of Sciences*, *108*(1), 67–72.